Vortex filament motion under the localized induction approximation in terms of Weierstrass elliptic functions

H. J. Shin*
Department of Physics and Research Institute of Basic Science, Kyung Hee University, Seoul 130-701, Korea
(Received 13 September 2001; published 6 March 2002)

We study quasiperiodic solutions of the localized induction approximation in terms of the elliptic functions of Weierstrass. They describe the Kida-class motion of a thin vortex filament in an incompressible inviscid fluid. Our solution includes various filament shapes such as the vortex ring, the helicoidal filament, the plane sinusoidal filament, and the Hasimoto type-1 soliton filament.

DOI: 10.1103/PhysRevE.65.036317 PACS number(s): 47.32.Cc, 47.15.Ki, 02.30.Gp

I. INTRODUCTION

The dynamics of a thin vortex filament in an incompressible inviscid fluid was first studied by Da Rios [1] and more recently by Hama [2]. They derived the so-called localized induction approximation (LIA) and used it to investigate the motion of filaments of various shape. In particular, Hasimoto [3] has proven the integrability of the LIA by identifying the vortex equation with the nonlinear Schrödinger equation (NSE). He also obtained a localized twist wave solution of the LIA which corresponds to the one-soliton solution of NSE. This solution was named the "Hasimoto soliton." See the review by Ricca [4,5] for a detailed account of the history and development of the LIA and related ideas discussed in the present paper. Experimentally, Hopfinger *et al.* [6] observed twisting distortions of a slender vortex tube in a rotating tank which resembled the Hasimoto soliton. In an additional experiment, these distortions were found to be stable against a collision [7]. These observations motivated studies on the *N*-soliton solutions of the LIA using the theory of soliton surfaces [8] and the Hirota method [9].

On the other hand, Kida [10] was able to obtain various vortex filaments which move steadily without deformation using a simple but interesting ansatz. They are expressed in terms of elliptic integrals which correspond to the traveling wave solution of the NSE. For some special values of parameters, Kida's solution reduces to the previously known shapes, for example, a circular ring, the Kelvin wave, a helicoidal filament, and the Hasimoto soliton. Unfortunately, the case of the *N*-soliton solutions ($N\geqslant 2$) was inaccessible by this technique. In fact, the traveling wave solution, which corresponds to Kida's solution of the LIA, is the simplest case of the so-called (quasi)periodic solutions of the NSE [11]. However, the construction of general periodic solutions of the LIA using the Hasimoto map and the periodic solutions of the NSE is a highly nontrivial task and has not been achieved yet. The application of the soliton surface theory to this problem can be an effective but also nontrivial task, and only expressions describing localized excitations of the Kida solution were obtained [12].

In this paper, we apply the "finite-band integration method" to find periodic solutions of the LIA. In mathematical literature, the problem of finding the periodic solutions of integrable equations has been considered for a long time. It was solved first for the case of the Korteweg–de Vries equation and was extended to the case of the sine-Gordon equation and the nonlinear Schrödinger equation later on [11]. This method is based upon the theory of the eigenvalue problem of the one-dimensional Schrödinger equation with a periodic potential. An important class of periodic potentials consists of those which generate only a finite number of nondegenerate eigenvalues, and these are called finite band potentials which give periodic solutions.

The following steps are known to be the simplest method for generating periodic solutions. We first express the integrable equation as a compatibility condition of two linear systems. It is known that this condition has a natural geometric interpretation and is called a zero-curvature representation. As we deal with the LIA directly rather than the NSE, we develop the zero-curvature formalism of the LIA which is explained in the Appendix. Then we introduce the "squared" eigenfunctions, which are known to simplify many of the computations. In the course of doing this, we obtain a system of partial differential equations on a set of auxiliary variables as well as those of the LIA, whose solution is connected with Jacobi's inversion problem [13]. Finally, these equations are solved using parameters that determine the periods and amplitudes of the solution and are called the main spectra. An explicit one-phase periodic solution is constructed using the Weierstrass elliptic functions. Various vortex filaments are analyzed by reducing the solution to the special degenerate limit.

The parameters of our solution are more explicit and easy to manipulate compared to Kida's solution. The present approach does not employ the ansatz of stationary filament configurations. It also offers a formal method to find a much wider class of solutions of the LIA encompassing the *N*-phase solutions. Explicit accomplishment of Jacobi's problem with the help of complex analysis on a Riemann surface would result in a solution expressed in closed form in terms of the Riemann θ functions. But there arises a technical difficulty in this program, which was called the "effectivization" problem in [15]. The problem is that the reality condition of the solution should be satisfied, which imposes some constraints on the auxiliary variables that appear in the

*Email address: hjshin@khu.ac.kr

theory. A simple technique was developed to overcome this difficulty. But this technique is still confined to the one-phase solution of the problem having only four spectral parameters. This difficulty and the complexity in treating the Riemann θ functions limit the availability of explicit solutions in the present paper. We plan to report the treatment of more general solutions, using numerical methods at least, in a separate paper.

In Sec. II, we review the localized induction approximation and introduce its Lax pair. The development of the zero-curvature formalism of the LIA in a suitable form for applying to the finite band integration method is explained in the Appendix. Explicit construction of the one-phase periodic solution is followed using a modified version of the finite integration method in Sec. III. The resulting formulas involve Weierstrass' elliptic functions. In Sec. IV, various vortex configurations from the periodic solutions are explained in terms of functional relations of the Weierstrass functions. In particular, the reduction of the solution to typical vortex motions is achieved. Section V contains a discussion.

II. LOCALIZED INDUCTION APPROXIMATION

Da Rios and lately Hama have shown that the nonrelativistic motion of a thin vortex filament of fluid mechanics is described by the so-called localized induction approximation:

$$\partial_\tau X^i = \epsilon_{ijk} \partial_\sigma X^j \partial_\sigma^2 X^k, \quad i=1,2,3, \tag{1}$$

where σ is the arc length and τ is the time. Here, $X^i(\sigma,\tau)$, $i=1,2,3$ are the vortex coordinates which satisfy the quadratic constraints:

$$(\partial_\sigma X^i)^2 = 1. \tag{2}$$

The localized induction approximation can be equally described in a matrix form, which is suitable for the dualization procedure with the nonlinear Schrödinger equation. Let us define a matrix X by

$$X \equiv \sum_{i=1}^{3} X^i \sigma_i, \tag{3}$$

where σ_i are Pauli matrices. Then it is easy to verify that the matrix X satisfies the following equation of motion:

$$\bar{\partial} X = \frac{1}{2i}[\partial X, \partial^2 X], \tag{4}$$

where $\partial \equiv \partial/\partial z, \bar{\partial} \equiv \partial/\partial \bar{z}, z \equiv \sigma, \bar{z} \equiv \tau$. The constraint equation (2) can also be rewritten with X as

$$\mathrm{Tr}(\partial X)^2 = 2. \tag{5}$$

First we notice that the equation of motion (4) can be rewritten as a zero-curvature condition

$$[\partial + i\lambda \partial X, \bar{\partial} - 2i\lambda^2 \partial X + i\lambda \bar{\partial} X] = 0, \tag{6}$$

where λ is an arbitrary spectral parameter. In turn, this zero-curvature condition can be understood as the integrability condition of the linear system,

$$(\partial + U)\Phi = 0, \quad (\bar{\partial} + V)\Phi = 0, \tag{7}$$

where

$$U = i\lambda \partial X \equiv i\lambda \begin{pmatrix} \alpha_3 & \alpha_+ \\ \alpha_- & -\alpha_3 \end{pmatrix},$$

$$\begin{aligned} V &= -2i\lambda^2 \partial X + i\lambda \bar{\partial} X \\ &\equiv -2i\lambda^2 \begin{pmatrix} \alpha_3 & \alpha_+ \\ \alpha_- & -\alpha_3 \end{pmatrix} + i\lambda \begin{pmatrix} \beta_3 & \beta_+ \\ \beta_- & -\beta_3 \end{pmatrix}, \end{aligned} \tag{8}$$

where $\alpha_+^* = \alpha_-$, $\alpha_3^* = \alpha_3$, $\beta_+^* = \beta_-$, $\beta_3^* = \beta_3$. The equation of motion (4) is rewritten as

$$2i\beta_3 = \alpha_+ \partial \alpha_- - \alpha_- \partial \alpha_+,$$

$$2i\beta_\pm = \pm 2\alpha_3 \partial \alpha_\pm \mp 2\alpha_\pm \partial \alpha_3, \tag{9}$$

while the constraint (5) becomes $\alpha_3^2 + \alpha_+ \alpha_- = 1$. We obtain the linear equation (7) using the so-called R transformation [14], which is explained in the Appendix. As we will see in the next section, this form is well-suited for the finite-band integration method.

III. FINITE-BAND INTEGRATION METHOD

We start with the linear equation (7). Let the systems (7) have two basic solutions, (ψ_1, ψ_2) and (ϕ_1, ϕ_2), which are used to build a vector such that

$$f = -(i/2)(\psi_1 \phi_2 + \psi_2 \phi_1), \quad g = \psi_1 \phi_1, \quad h = -\psi_2 \phi_2. \tag{10}$$

Using this definition and the linear equation (7), it can be explicitly checked that $P(\lambda) \equiv f^2 - gh$ is independent of z and $\bar{z}$ and is only the function of λ. The N-phase periodic solution is obtained by specially taking the form of

$$P(\lambda) = f^2 - gh = \prod_{i=1}^{2N+2} (\lambda - \lambda_i), \tag{11}$$

where λ_i are zeros of the polynomial which characterize the periodic solution of the "Bloch wave" problem and are called the main spectra. The zeros λ_i have to consist of complex conjugate pairs $\lambda_j = \lambda_{Rj} + i\lambda_{Ij}$, $\lambda_{j+N+1} = \lambda_{Rj} - i\lambda_{Ij}$, $j = 1, N+1$ such that the obtained solutions $\mathbf{X}_i, i = 1,3$ are real. It can be seen that this form is consistent with the following form of f, g, and h,

$$f = \alpha_3 \lambda^{N+1} + \sum_{i=0}^{N} \lambda^i f_i,$$

$$g = -i\lambda\alpha_+ \prod_{i=1}^{N} (\lambda - \mu_i), \tag{12}$$

$$h = -i\lambda\alpha_- \prod_{i=1}^{N} (\lambda - \mu_i^*),$$

where μ_i are functions of $z,\bar{z}$. From the definition of f, g, and h in Eq. (10), we can obtain the following equations:

$$\partial f = -\lambda\alpha_- g + \lambda\alpha_+ h, \quad \partial g = 2\lambda\alpha_+ f - 2i\lambda\alpha_3 g,$$

$$\bar{\partial} f = 2\lambda^2\alpha_- g - 2\lambda^2\alpha_+ h - \lambda\beta_- g + \lambda\beta_+ h, \tag{13}$$

$$\bar{\partial} g = -4\lambda^2\alpha_+ f + 4i\lambda^2\alpha_3 g + 2\lambda\beta_+ f - 2i\lambda\beta_3 g.$$

Equations for h are similarly given.

If we evaluate Eq. (11) at μ_m, which is one of the zeros of g, then we arrive at the identity

$$f(z,\bar{z};\mu_m) = \sigma_m\sqrt{P(\mu_m)}, \tag{14}$$

where σ_m indicates the sheet of the Riemann surface on which the complex μ_m lies. Using Eqs. (12) and (13), we can evaluate ∂g at one of the zeros of g to find

$$\partial\mu_m = -2i\sigma_m\sqrt{P(\mu_m)}/\prod_{i\neq m} (\mu_m - \mu_i), \quad m = 1, \ldots, N. \tag{15}$$

If we look at the λ^{N+1} term for ∂f in Eq. (13), we find

$$\partial\alpha_3 = -i\alpha_+\alpha_- \sum_i (\mu_i - \mu_i^*) = -i(1-\alpha_3^2)\sum_i (\mu_i - \mu_i^*). \tag{16}$$

Now the $O(\lambda^{2N+1})$ term of $P(\lambda)$ gives

$$2\alpha_3 f_N - \alpha_+\alpha_- \sum (\mu_i + \mu_i^*) = -\sum \lambda_i \tag{17}$$

and the $O(\lambda^{N+1})$ term of the second of Eqs. (13) gives

$$\partial\alpha_+ = 2i\alpha_+ f_N + 2i\alpha_3\alpha_+ \sum \mu_i. \tag{18}$$

Using these results, we obtain

$$\beta_+ = 2\alpha_3\alpha_+ f_N + 2\alpha_3^2\alpha_+ \sum \mu_i + \alpha_+^2\alpha_- \sum (\mu_i - \mu_i^*)$$
$$= \left(-\sum \lambda_i + 2\sum \mu_i\right)\alpha_+. \tag{19}$$

Applying the same approach to $\bar{\partial} g$ and $\bar{\partial} f$ in Eqs. (13) and using the results in Eq. (19), we can show

$$\bar{\partial}\mu_m = 2i\left(2\mu_m - \frac{\beta_+}{\alpha_+}\right)\sigma_m\sqrt{P(\mu_m)}/\prod_{i\neq m} (\mu_m - \mu_i)$$
$$= 2i\left(\sum \lambda_i - 2\sum \mu_i + 2\mu_m\right)$$
$$\times\sigma_m\sqrt{P(\mu_m)}/\prod_{i\neq m} (\mu_m - \mu_i), \tag{20}$$

$$\bar{\partial}\alpha_3 = -2i\alpha_+\alpha_- \sum_{i>j} (\mu_i\mu_j - \mu_i^*\mu_j^*)$$
$$- i\alpha_+\beta_- \sum \mu_i + i\alpha_-\beta_+ \sum \mu_i^*$$
$$= i\alpha_+\alpha_- \left\{-2\sum_{i>j} (\mu_i\mu_j - \mu_i^*\mu_j^*)\right.$$
$$\left. + \sum \lambda_i \sum (\mu_i - \mu_i^*)\right\}\alpha_+\alpha_-. \tag{21}$$

The remaining problem to solve Eqs. (15)–(21) is beautifully accomplished by using the solution of what is called Jacobi's inversion problem. We will not go into details here but sketch the broad outlines and occurring difficulties of the procedure. The following steps are needed to solve the above problem. First, take the parameters λ_i, $i = 1, \ldots, 2N+2$ as known. Second, choose initial conditions $\mu_i(0,0)$ and $\alpha_3(0,0)$ such that they satisfy Eq. (11). It is at this point that a technical difficulty arises. An effective method to avoid this problem was introduced by Kamchatnov [15] to obtain the one-phase solution. We adopt this method in the following section to obtain an explicit periodic solution of the string configuration.

IV. ONE-PHASE PERIODIC SOLUTION

As explained in the previous section, in the sine-Gordon and NLS equations, the additional problem of extraction of the "real" solutions arises. The periodic solutions obtained by this method have a rather complicated form, which prevents their application to real physical situations. Kamchatnov devised a simple modification of the finite-band integration method which solves the so-called "effectivization" problem in the simplest and the important one-phase case. In this section, we follow his method to find the periodic solutions of the localized induction approximation. The one-phase periodic solution is obtained by taking the simplest nontrivial $N=1$ case in Eqs. (11) and (12), which gives

$$P(\lambda) = \prod_{i=1}^{4} (\lambda - \lambda_i), \quad f = \alpha_3\lambda^2 + f_1\lambda + f_0,$$

$$g = -i\lambda\alpha_+(\lambda - \mu), \quad h = -i\lambda\alpha_-(\lambda - \mu^*). \tag{22}$$

Equation (17) then becomes

$$2\alpha_3 f_1-\alpha_+\alpha_-(\mu+\mu^*)=-\sum \lambda_i. \tag{23}$$

Here we define

$$V\equiv-\sum \lambda_i. \tag{24}$$

The other equations from Eq. (13) for the $N=1$ case can be expressed as

$$\partial\alpha_3=-i\alpha_+\alpha_-(\mu-\mu^*),\quad \partial f_1=\partial f_0=0,$$

$$\partial\mu=-2i(\alpha_3\mu^2+f_1\mu+f_0), \tag{25}$$

$$\bar\partial\alpha_3=V\partial\alpha_3,\quad \bar\partial f_1=\bar\partial f_0=0,\quad \bar\partial\mu=V\partial\mu,$$

$$\partial\alpha_+=2i\alpha_+f_1+2i\alpha_3\alpha_+\mu,\quad \bar\partial\alpha_+=-4if_0\alpha_++V\partial\alpha_+.$$

Note that α_3 and μ are functions of $W\equiv z+V\bar z$ only and f_0,f_1 are constants.

A. μ, f_1, f_0 in terms of α_3, s_i

To prevent the ''effectivization'' problem, we start with Eq. (11) or Eq. (22) to solve μ, f_1, and f_0. First, we introduce constants of motion s_i, $i=1,4$, which are defined as

$$P(\lambda)=f^2-gh=\lambda^4-s_1\lambda^3+s_2\lambda^2-s_3\lambda+s_4. \tag{26}$$

Inserting f, g, and h in Eq. (22) into Eq. (26), we can obtain

$$s_1\equiv\sum \lambda_i=-2f_1\alpha_3+X,$$

$$s_2\equiv\sum_{i<j} \lambda_i\lambda_j=2f_0\alpha_3+f_1^2+Y, \tag{27}$$

$$s_3\equiv\sum_{i<j<k} \lambda_i\lambda_j\lambda_k=-2f_1f_0,\qquad s_4\equiv\prod \lambda_i=f_0^2,$$

where $X\equiv\alpha_+\alpha_-(\mu+\mu^*)=(1-\alpha_3^2)(\mu+\mu^*)$ and $Y\equiv\alpha_+\alpha_-\mu\mu^*$. Now solving for f_0, f_1, μ, and μ^* in Eq. (27), we obtain[1]

$$f_1=\frac{s_3}{2\sqrt{s_4}},\qquad f_0=-\sqrt{s_4},$$

$$\mu,\mu^*=\frac{1}{2(1-\alpha_3^2)s_4}(\sqrt{s_4}s_3\alpha_3+s_1s_4\mp\sqrt{s_4R}), \tag{28}$$

where

$$R=(x+\lambda_2\lambda_3+\lambda_1\lambda_4)(x+\lambda_1\lambda_3+\lambda_2\lambda_4)\times(x+\lambda_1\lambda_2+\lambda_3\lambda_4),$$

$$x=2\sqrt{s_4}\alpha_3. \tag{29}$$

Note that this solution is consistent with Eq. (25).

B. Derivation of X_3

Using these results, Eq. (25) for α_3 becomes

$$\frac{d\alpha_3}{dW}=\frac{i}{\sqrt{s_4}}\sqrt{R}. \tag{30}$$

This equation can be integrated in terms of Weierstrass' $\mathcal{P}(u,g_2,g_3)$ function. As far as Weierstrass elliptic functions are involved, we employ the terminology and notation of Ref. [16] without further explanations. Explicitly

$$\alpha_3=\frac{1}{2\sqrt{s_4}}\left(-\frac{s_2}{3}-\mathcal{P}(W+w_3,g_2,g_3)\right), \tag{31}$$

where w_3 is an integration constant and $g_2=\frac{4}{3}s_2^2-4s_1s_3+16s_4$, $g_3=\frac{8}{27}s_2^3-\frac{4}{3}s_1s_2s_3+4s_3^2-\frac{32}{3}s_2s_4+4s_1^2s_4$. The integration constant w_3 is determined by the initial condition, which we shall choose as follows: $\mathcal{P}(w_3)=e_3$ at $W=0$, where e_3 is the smallest root of the equation $4z^3-g_2z-g_3=0$. [Two other roots are denoted by e_1 and e_2 with $e_1>e_2>e_3$. w_3 as well as w_1 are called the half-period of the $\mathcal{P}$ function. They satisfy $\mathcal{P}(w_1)=e_1,\mathcal{P}(w_2)=e_2,e_1+e_2+e_3=w_1+w_2+w_3=0$.] This condition guarantees $|\alpha_3|\leqslant 1$. Now using $\alpha_3=\partial X_3$ and $\beta_3=\bar\partial X_3=-s_3/\sqrt{s_4}+V\partial X_3$, we can obtain

$$X_3=\int \alpha_3 dW-s_3/\sqrt{s_4 z}$$
$$=\frac{1}{2\sqrt{s_4}}\left\{\zeta(W+w_3,g_2,g_3)-\frac{s_2}{3}W-2s_3\bar z-\eta_3\right\}, \tag{32}$$

where $\zeta(u,g_2,g_3)$ is the Weierstrass' zeta function and the integration constant η_3 is taken as $\zeta(w_3,g_2,g_3)$. [We will use the notation $\eta_i=\zeta(w_i,g_2,g_3),i=1,3$ in the following.]

C. Derivation of α_+

Now we try to obtain the solution X_+ of the localized induction approximation. Using Eq. (28), we can solve the last two equations of Eqs. (25) for α_+, which becomes

$$\alpha_+=\exp(4\sqrt{s_4}i\bar z)\tilde\alpha_+(W), \tag{33}$$

[1] This is one particular solution, but other solutions give essentially the same result. To obtain this solution, we use MATHEMATICA for symbolic manipulation. In addition, MATHEMATICA was used to check various formulas appearing in this paper. For example, it was used to check that Eqs. (32) and (48) satisfy the equation of motion (4).

where $\tilde{\alpha}_+$ satisfies the following differential equation:

$$\frac{d\tilde{\alpha}_+}{dW}=2i\tilde{\alpha}_+(f_1+\alpha_3\mu). \tag{34}$$

The following identity, which can be obtained using Eqs. (28) and (30), is required to integrate $\tilde{\alpha}_+$:

$$\begin{aligned}2i(f_1+\alpha_3\mu)&=\frac{i}{(1-\alpha_3^2)\sqrt{s_4}}(s_3+s_1\sqrt{s_4}\alpha_3)\\&\quad+\frac{1}{2}\frac{d(1-\alpha_3^2)}{(1-\alpha_3^2)dW}\\&=iM_1\frac{1}{1+\alpha_3}+iM_2\frac{1}{1-\alpha_3}+\frac{1}{2}\frac{d(1-\alpha_3^2)}{(1-\alpha_3^2)dW},\end{aligned} \tag{35}$$

where

$$M_1,M_2=\frac{s_3}{2\sqrt{s_4}}\mp\frac{s_1}{2}. \tag{36}$$

Now using Eqs. (31),(34),(35) and the following identities of the Weierstrass' elliptic function:

$$\int\frac{dW}{\mathcal{P}(W)-\mathcal{P}(\kappa)}=\frac{1}{\mathcal{P}'(\kappa)}\left\{\ln\frac{\sigma(\kappa-W)}{\sigma(\kappa+W)}+2\zeta(\kappa)W\right\} \tag{37}$$

and

$$\mathcal{P}(W)-\mathcal{P}(\kappa)=-\frac{\sigma(W+\kappa)\sigma(W-\kappa)}{\sigma^2(W)\sigma^2(\kappa)}, \tag{38}$$

we can obtain

$$\begin{aligned}\tilde{\alpha}_+&=\frac{i}{2\sqrt{s_4}}\frac{\sigma(W+w_3+\kappa_1)\sigma(W+w_3+\kappa_2)}{\sigma(\kappa_1)\sigma(\kappa_2)\sigma^2(W+w_3)}\\&\quad\times\exp\{-\zeta(\kappa_1)W-\zeta(\kappa_2)W+c\},\end{aligned} \tag{39}$$

where two constants κ_1,κ_2 are defined by the following two relations:

$$\mathcal{P}(\kappa_1),\mathcal{P}(\kappa_2)=-s_2/3\pm2\sqrt{s_4}, \tag{40}$$

$$\begin{aligned}\mathcal{P}'(\kappa_1),\mathcal{P}'(\kappa_2)&=-2\sqrt{s_4}\frac{d\alpha_3}{dW}\Big|_{\alpha_3=\mp1}=-2i\sqrt{R}\Big|_{\alpha_3=\mp1}\\&=-2i(s_1\sqrt{s_4}\mp s_3)=\pm4\sqrt{s_4}iM_{1,2}.\end{aligned} \tag{41}$$

We fix the integration constant c by requiring $\alpha_3^2+|\alpha_+|^2=1$. Especially at $W=0$, we find

$$\begin{aligned}\alpha_3(0)&=\frac{1}{2\sqrt{s_4}}\left(-\frac{s_2}{3}-e_3\right)\\&=\frac{1}{2\sqrt{s_4}}\left(\frac{\mathcal{P}(\kappa_1)+\mathcal{P}(\kappa_2)}{2}-e_3\right),\end{aligned}$$

$$\begin{aligned}\tilde{\alpha}_+(0)&=\frac{i}{2\sqrt{s_4}}\frac{\sigma(\kappa_1+w_3)\sigma(\kappa_2+w_3)}{\sigma(\kappa_1)\sigma(\kappa_2)\sigma^2(w_3)}\exp(c)\\&=\frac{-1}{2\sqrt{s_4}}\sqrt{[\mathcal{P}(\kappa_1)-e_3][-\mathcal{P}(\kappa_2)+e_3]}\\&\quad\times\exp\{\zeta(w_3)(\kappa_1+\kappa_2)+c\},\end{aligned} \tag{42}$$

where we have used the identity

$$\mathcal{P}(u)-e_3=\frac{\sigma^2(u+w_3)}{\sigma^2(u)\sigma^2(w_3)}\exp\{-2\zeta(w_3)u\}. \tag{43}$$

Using these relations together with Eq. (40), we can obtain $c=-\eta_3(\kappa_1+\kappa_2)$.

D. Derivation of X_+

We now derive X_+. Using $\partial X_+=\alpha_+$ in Eq. (8), we obtain

$$X_+=\int\alpha_+dz+M(\bar{z})=\exp(4\sqrt{s_4}i\bar{z})\int\tilde{\alpha}_+dW+M(\bar{z}), \tag{44}$$

where $M(\bar{z})$ is a function to be determined. To evaluate the integration explicitly and to determine $M(\bar{z})$, we substitute Eq. (44) into the following equation:

$$\bar{\partial}X_+=\beta_+=(-s_1+2\mu)\alpha_+. \tag{45}$$

Then a little algebra with Eqs. (28), (30), (31), (33), (39), (40), and (41) gives $M(\bar{z})=0$ and

$$\begin{aligned}4\sqrt{s_4}i\int\tilde{\alpha}_+dW&=\frac{1}{\alpha_+\alpha_-}\left(\frac{s_3}{\sqrt{s_4}}\alpha_3+s_1-\sqrt{\frac{R}{s_4}}\right)\tilde{\alpha}_+=\frac{i}{2}\left(\frac{\mathcal{P}'(W+w_3)-\mathcal{P}'(\kappa_1)}{\mathcal{P}(W+w_3)-\mathcal{P}(\kappa_1)}-\frac{\mathcal{P}'(W+w_3)-\mathcal{P}'(\kappa_2)}{\mathcal{P}(W+w_3)-\mathcal{P}(\kappa_2)}\right)\tilde{\alpha}_+\\&=-\frac{1}{2\sqrt{s_4}}\{\zeta(W+w_3+\kappa_1)-\zeta(W+w_3+\kappa_2)-\zeta(\kappa_1)+\zeta(\kappa_2)\}\frac{\sigma(W+w_3+\kappa_1)\sigma(W+w_3+\kappa_2)}{\sigma(\kappa_1)\sigma(\kappa_2)\sigma^2(W+w_3)}\\&\quad\times\exp\{-\zeta(\kappa_1)W-\zeta(\kappa_2)W-\eta_3(\kappa_1+\kappa_2)\},\end{aligned} \tag{46}$$

where we use the following relation in the last part of the derivation:

$$\frac{\mathcal{P}'(W)-\mathcal{P}'(\kappa)}{\mathcal{P}(W)-\mathcal{P}(\kappa)}=2\zeta(W+\kappa)-2\zeta(W)-2\zeta(\kappa). \tag{47}$$

Thus collecting all these results, we finally obtain

$$X_+=\frac{i}{8s_4}\{\zeta(W+w_3+\kappa_1)-\zeta(W+w_3+\kappa_2)-\zeta(\kappa_1)+\zeta(\kappa_2)\}\frac{\sigma(W+w_3+\kappa_1)\sigma(W+w_3+\kappa_2)}{\sigma(\kappa_1)\sigma(\kappa_2)\sigma^2(W+w_3)}\exp\{-\zeta(\kappa_1)W-\zeta(\kappa_2)W-\eta_3(\kappa_1+\kappa_2)+4\sqrt{s_4}i\overline{z}\}. \tag{48}$$

V. SPECIAL CASES

In this section, we study some special cases of the obtained solution by taking the degenerate limit of the λ_i values. It contains the straight line, the Kelvin wave, and the Hasimoto soliton solution, which were obtained previously, as well as such new configurations as the plane curve, the closed ring, and the point particle.

A. Straight line

The simplest solution that corresponds to the straight line is obtained by taking $\lambda_1=\lambda_3=\alpha$, $\lambda_2=\lambda_4=\gamma$, or more simply $\lambda_1=\lambda_2=\lambda_3=\lambda_4=\alpha$ (real). In this case, $g_2=g_3=e_3=0$. The Weierstrass functions in this limit are given by $\mathcal{P}(u,0,0)=1/u^2$, $\zeta(u,0,0)=1/u$, $\sigma(u,0,0)=u$, and $w_3=\kappa_1=\infty$. Using these relations, we can easily obtain $X_3=-z, X_+=X_1-iX_2=0$. The rotational and translational symmetry of the vortex equation can give a more general configuration of the straight line [20].

B. Kelvin wave or smoke ring

The next example, known as the Kelvin wave, corresponds to taking $\lambda_1=\lambda_3=\alpha$, $\lambda_2=\alpha+i\gamma$, and $\lambda_4=\alpha-i\gamma$ $(0<\alpha<1,\ 0<\gamma)$. In this case $g_2=\frac{4}{3}\gamma^4, g_3=\frac{8}{27}\gamma^6$. As $\Delta\equiv g_2^3-27\gamma_3^2=0$, the Weierstrass functions are given in a simple form,

$$\mathcal{P}(u)=-\gamma^2/3+\gamma^2\csc^2(\gamma u),$$
$$\zeta(u)=\gamma^2u/3+\gamma\cot(\gamma u), \tag{49}$$
$$\sigma(u)=\exp(\gamma^2u^2/6)\sin(\gamma u)/\gamma,$$

and $e_3=-\gamma^2/3$, $w_3=i\infty$,

$$\sin\gamma\kappa_1,\sin\gamma\kappa_2=\sqrt{\frac{\gamma^2}{\pm2\alpha\sqrt{\alpha^2+\gamma^2}-2\alpha^2}}, \tag{50}$$

$$\cot\gamma\kappa_1,\cot\gamma\kappa_2=-\frac{i}{\gamma}(\sqrt{\alpha^2+\gamma^2}\mp\alpha). \tag{51}$$

Now, a straightforward calculation gives

$$X_3=-\frac{1}{\sqrt{\alpha^2+\gamma^2}}(\alpha z+2\gamma^2\overline{z}),$$

$$X_+=i\frac{\gamma}{2(\alpha^2+\gamma^2)}\exp[2i\sqrt{\alpha^2+\gamma^2}(z-2\alpha\overline{z})]. \tag{52}$$

Using the fact that $X_+=X_1-iX_2\equiv iC\exp(iD)$, we can obtain $X_1=(X_++X_+^*)/2=-C\sin D$ and $X_2=i(X_+-X_+^*)/2=-C\cos D$, which describes a smoke ring. When $\alpha=0$, it describes a circular ring having a constant radius and traveling along the z axis. When $\alpha\neq0$, it describes a helicoidal filament with the radius $\gamma/(2\alpha^2+2\gamma^2)$ and the pitch $-\alpha\pi$. The helix rotates with the angular velocity $-4\alpha\sqrt{\alpha^2+\gamma^2}$ around the z axis and moves with a speed $-2\gamma^2/\sqrt{\alpha^2+\gamma^2}$ in the z direction. This solution is first discussed in [21].

C. Hasimoto one-soliton solution

To obtain the one-soliton solution from our periodic solution, we take $\lambda_1=\lambda_2=\alpha+i\gamma$, $\lambda_3=\lambda_4=\alpha-i\gamma$ in Eqs. (32) and (48). In this case, $g_2=\frac{64}{3}\gamma^4, g_3=-\frac{512}{27}\gamma^6$, and $w_3=i\pi/(4\gamma)$, $e_3=\mathcal{P}(w_3)=-8\gamma^2/3$, $\eta_3=\zeta(w_3)=-i\gamma\pi/3$, and $\sigma(w_3)=i\exp(\pi^2/24)/(2\gamma)$. The Weierstrass functions are given by

$$\mathcal{P}(W+w_3)=-8\gamma^2/3+4\gamma^2\tanh^2(2\gamma W),$$
$$\zeta(W+w_3)=-4\gamma^2W/3+2\gamma\tanh(2\gamma W)+\eta_3, \tag{53}$$
$$\sigma(W+w_3)=\exp(-2\gamma^2W^2/3+\eta_3W)\times\cosh(2\gamma W)\sigma(w_3),$$

and $\kappa_1=\infty$, $\sinh2\gamma\kappa_2=i\gamma/\sqrt{\alpha^2+\gamma^2}$, $\coth2\gamma\kappa_2=-i\alpha/\gamma$, and $\eta_3=-i\gamma\pi/3, \sigma(w_3)=i\exp(\pi^2/24)/(2\gamma)$. It then gives

$$X_3=-z+\frac{\gamma}{\alpha^2+\gamma^2}\tanh\{2\gamma(z-4\alpha\overline{z})\} \tag{54}$$

and

$$X_+=-\frac{i\gamma}{\alpha^2+\gamma^2}\operatorname{sech}(2\gamma W)\exp\{2i\alpha z-4i(\alpha^2-\gamma^2)\overline{z}\}. \tag{55}$$

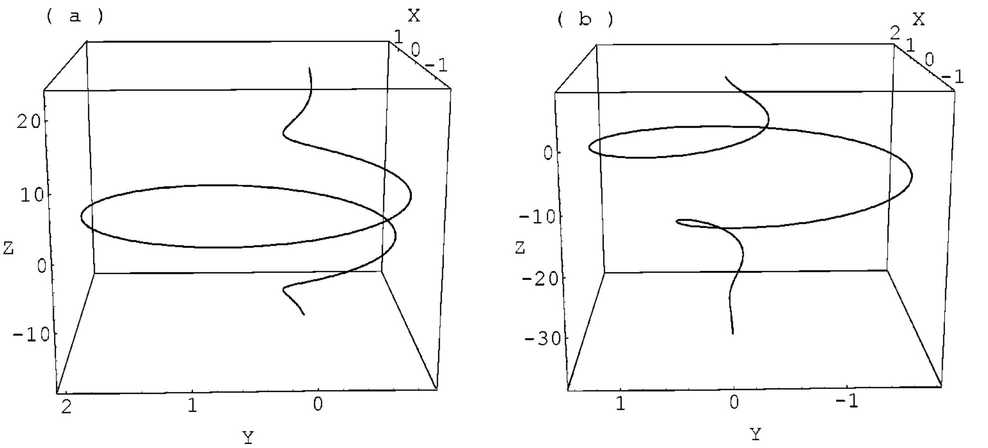

FIG. 1. A typical soliton vortex filament drawn with (a) $-25<\sigma<20$ at $\tau=0$ and (b) $-10<\sigma<40$ at $\tau=10$. The parameters of the vortex filament are $\alpha=0.2, \gamma=0.1$.

This solution can be compared with the known form in [10] by taking $\lambda_1=\lambda_2=\lambda_3^*=\lambda_4^*\to(C_{\mathrm{Kida}}+I\sqrt{\alpha_{\mathrm{Kida}}})/4$. In Fig. 1, we show one example of the Hasimoto vortex filament with $\alpha=0.2, \gamma=0.1$.

D. Rigid vortex filament

When we take $\lambda_1=\lambda_3^*=\alpha+i\gamma_1, \lambda_2=\lambda_4^*=-\alpha+i\gamma_2$, then $\Sigma\lambda_i=0$ and $W=(z-\Sigma\lambda_i\bar{z})$ becomes z. As we can see in the following, it gives a configuration of type $X_1=a(\sigma)\cos(b\tau)$, $X_2=a(\sigma)\sin(b\tau)$, and $X_3=c(\sigma)+d\tau$. Thus it describes a rigid filament which rotates around the z axis with constant angular velocity $[=4\sqrt{(\alpha^2+\gamma_1^2)(\alpha^2+\gamma_2^2)}]$ and moves along the z axis with constant velocity $[=-2\alpha(\gamma_2^2-\gamma_1^2)/\sqrt{(\alpha^2+\gamma_1^2)(\alpha^2+\gamma_2^2)}]$. This configuration might be interesting as it can be easily observed in experiments.

In this case,

$$g_2=\tfrac{4}{3}\{16\alpha^4+8(\gamma_1^2+\gamma_2^2)\alpha^2+\gamma_1^4+\gamma_2^4+14\gamma_1^2\gamma_2^2\},$$

$$\begin{aligned}g_3=\tfrac{8}{27}\{&64\alpha^6+48(\gamma_1^2+\gamma_2^2)\alpha^4\\&+12(\gamma_1^4+\gamma_2^4-10\gamma_1^2\gamma_2^2)\alpha^2+\gamma_1^6+\gamma_2^6-33\gamma_1^2\gamma_2^4\\&-33\gamma_1^4\gamma_2^2\}\end{aligned} \tag{56}$$

and

$$e_1=\tfrac{2}{3}(4\alpha^2+\gamma_1^2+\gamma_2^2),$$

$$e_2=\tfrac{1}{3}(-4\alpha^2-\gamma_1^2-\gamma_2^2+6\gamma_1\gamma_2), \tag{57}$$

$$e_3=\tfrac{2}{3}(-4\alpha^2-\gamma_1^2-\gamma_2^2-6\gamma_1\gamma_2).$$

Explicitly, the vortex filament is described by

$$\begin{aligned}X_3=&-\frac{\gamma_1^2+\gamma_2^2-2\alpha^2}{6\sqrt{H}}z+\frac{1}{2\sqrt{H}}\{\zeta(z+w_3,g_2,g_3)-\eta_3\}\\&-\frac{2\alpha(\gamma_2^2-\gamma_1^2)}{\sqrt{H}}\bar{z},\end{aligned}$$

$$\begin{aligned}X_+=&\frac{i}{8H}\{\zeta(z+w_3+\kappa_1)-\zeta(z+w_3+\kappa_2)\\&-\zeta(\kappa_1)+\zeta(\kappa_2)\}\\&\times\frac{\sigma(z+w_3+\kappa_1)\sigma(z+w_3+\kappa_2)}{\sigma(\kappa_1)\sigma(\kappa_2)\sigma^2(z+w_3)}\\&\times\exp\{\zeta(\kappa_1)z+\zeta(\kappa_2)z+4\sqrt{H}i\bar{z}-\eta_3(\kappa_1+\kappa_2)\},\end{aligned} \tag{58}$$

where $H=(\alpha^2+\gamma_1^2)(\alpha^2+\gamma_2^2)$.

E. Closed ring

The characteristics of closed rings can be studied using the following quasiperiodicity properties of Weierstrass' elliptic functions:

$$\zeta(u+2w_i)=\zeta(u)+2\eta_i,$$

$$\sigma(u+2w_i)=-\exp\{2\eta_i(u+w_i)\}\sigma(u). \tag{59}$$

As $w_1=K(\sqrt{(e_2-e_3)/(e_1-e_3)})/\sqrt{e_1-e_3}, w_3=iK(\sqrt{(e_1-e_2)/(e_1-e_3)})/\sqrt{e_1-e_3}$, w_1 is real while w_3 is pure imaginary. Thus physical characteristics are described by the real period $\Delta W=\Delta\sigma=2w_1$. For example, X_+ obtains an additional factor,

$$\exp\{2\eta_1(\kappa_1+\kappa_2)-2\zeta(\kappa_1)w_1-2\zeta(\kappa_2)w_1\} \tag{60}$$

after a period $\Delta W=2w_1$. Thus a necessary condition for a closed ring, i.e., $X_+(\sigma=m\Delta\sigma)=X_+(\sigma=0)$, is

$$\eta_1(\kappa_1+\kappa_2)-w_1\{\zeta(\kappa_1)+\zeta(\kappa_2)\}=i\frac{n}{m}\pi, \tag{61}$$

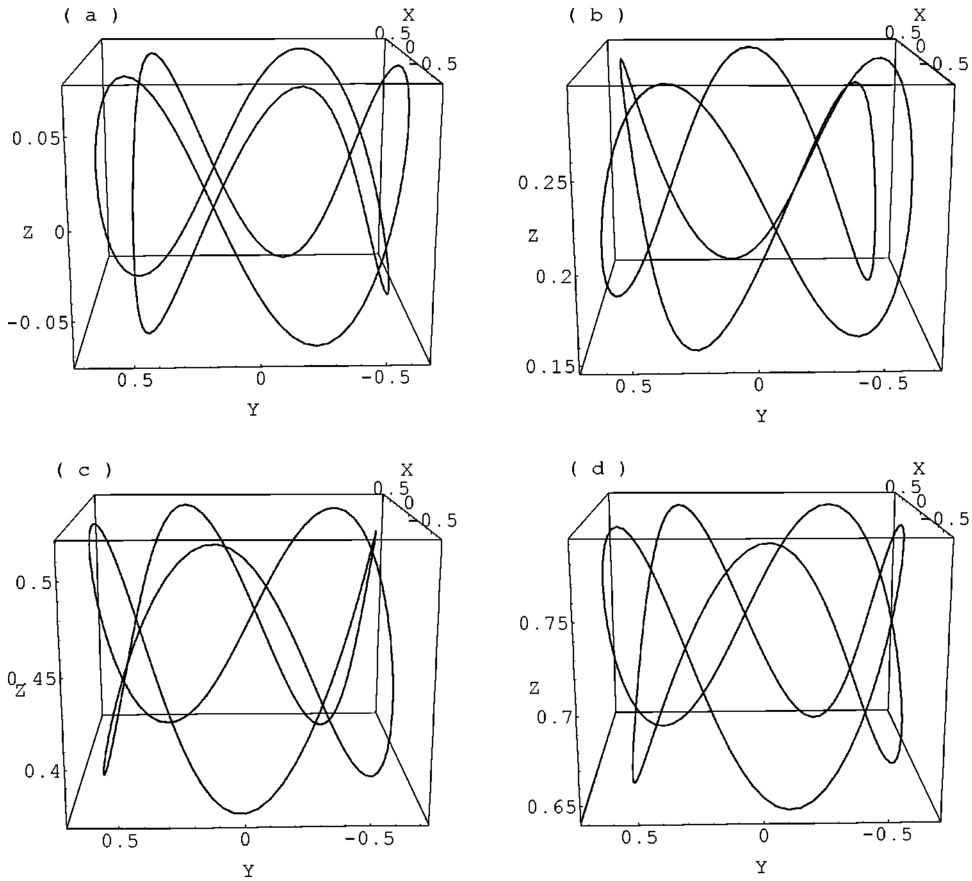

FIG. 2. A typical closed ring plotted for $-5<\sigma<5$ with parameters $\lambda_1=0.0126+0.8i$, $\lambda_2=-1.692+0.5i$ at (a) $\tau=0$, (b) $\tau=0.15$, (c) $\tau=0.3$, and (d) $\tau=0.484$ (time period).

where m,n are arbitrary integers. Another condition comes from the closedness of the z coordinate, i.e., $X_3(\sigma=m\Delta\sigma)=X_3(\sigma=0)$, which is

$$-\frac{s_2}{3\sqrt{s_4}}w_1+\frac{1}{\sqrt{s_4}}\eta_1=0, \tag{62}$$

i.e., $s_2 w_1=3\eta_1$.

The quasiperiodic property of the closed ring along the time is the following. During a time period $\Delta\tau=-2w_1/s_1$, the ring returns to its original shape but rotates around the z axis by an angle

$$\frac{2n}{m}\pi+4\sqrt{s_4}\Delta\tau, \tag{63}$$

and moves a distance

$$-\frac{s_3}{\sqrt{s_4}}\Delta\tau=\frac{2s_3w_1}{\sqrt{s_4}s_1} \tag{64}$$

along the z axis. The two conditions (61) and (62) can be solved numerically using a software package such as MATHEMATICA. For example, $\lambda_1=\lambda_3^*=0.0126+0.8i$, $\lambda_2=\lambda_4^*=-1.692+0.5i$ was found to be the solution of the conditions for a choice $n=2$, $m=5$. Figure 2 shows the motion of a closed ring at $\tau=0$, 0.15, 0.3, and 0.484 ($=\Delta\tau$, time period). During a time period $\Delta\tau$, the ring rotates -2.7336 rad and advances -0.716 along the z axis. The σ period is $\Delta\sigma=-1.626$ in this configuration.

F. Plane curve

The Weierstrass σ function appearing in the X_+ solution in Eq. (48) can be reduced to Jacobi's elliptic functions under a certain limit. For this, we first notice that

$$\frac{\sigma(W+w_3+\kappa_1)\sigma(W+w_3+\kappa_2)}{\sigma(W+w_3)^2}=\exp\left(\frac{\eta_1}{2w_1}\{\kappa_1^2+\kappa_2^2+2(\kappa_1+\kappa_2)(W+w_3)\}\right)\times\frac{H(\sqrt{e_1-e_3}(W+w_3+\kappa_1))H(\sqrt{e_1-e_3}(W+w_3+\kappa_2))}{H(\sqrt{e_1-e_3}(W+w_3))^2}, \tag{65}$$

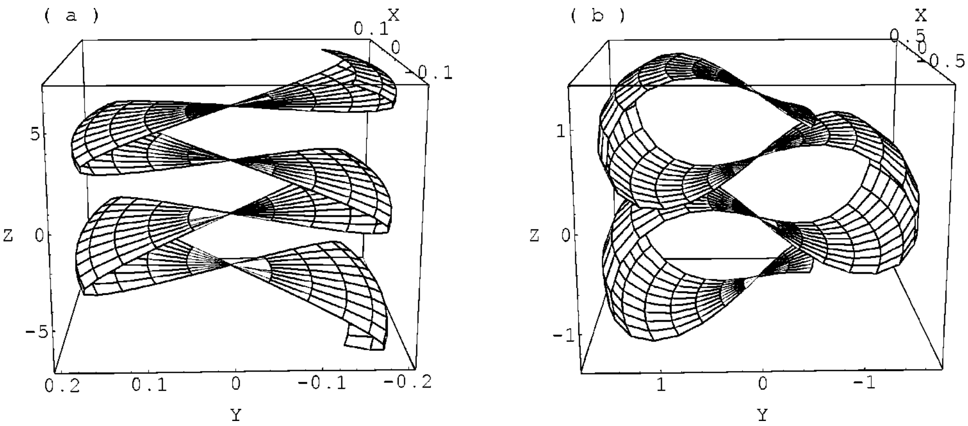

FIG. 3. Typical plane curves drawn with $\pi/3<\tau<2\pi/3$ and $-7<\sigma<7$. The parameters of the curves are $r=\frac{1}{2}$ and (a) $k=0.1$, (b) $k=0.85$.

where $H(u)\equiv\theta_1((\pi/2K)u)$. As $\mathrm{sn}\,u=(1/\sqrt{k})\,\theta_1(\pi u/2K)/\theta_4(\pi u/2K)$, $\mathrm{dn}u=\sqrt{k'}\,\theta_3(\pi u/2K)/\theta_4(\pi u/2K)$, and $\theta_1(u+(\pi/2))=\theta_2(u)$, $\theta_1(u+(\pi\tau/2))=iq^{-1/4}e^{-iu}\theta_4(u)$, it is required $(\pi/2K)\sqrt{e_1-e_3}\kappa_{1,2}\to\pi/2,\ \pi\tau/2$ to achieve our goal. In other words, $\kappa_{1,2}\to w_{1,3}$. Here we study the case $\kappa_1\to w_1,\kappa_2\to w_3$. The other case gives a similar result. Then $\mathcal{P}(\kappa_1)=2\sqrt{s_4}-s_2/3=\mathcal{P}(w_1)=e_1=\lambda_1\lambda_3+\lambda_2\lambda_4-s_2/3$ and $\mathcal{P}(\kappa_2)=-2\sqrt{s_4}-s_2/3=\mathcal{P}(w_3)=e_3=\lambda_1\lambda_2+\lambda_3\lambda_4-s_2/3$. To satisfy this condition, we choose $\lambda_1=\lambda_3^*=re^{i\theta}$, $\lambda_2=\lambda_4^*=-re^{-i\theta}$. With this choice, the expression in Eq. (65) becomes

$$\frac{\sigma(W+w_3+\kappa_1)\sigma(W+w_3+\kappa_2)}{\sigma(W+w_3)^2}=\exp\left(\frac{\eta_1}{2w_1}(w_1^2+w_3^2-2w_2w_3-2w_2W)\right)q^{-3/4}\times\exp\left(-i\frac{\pi}{2w_1}W\right)\sqrt{\frac{k}{k'}}\mathrm{sn}(\sqrt{e_1-e_3}W)\mathrm{dn}(\sqrt{e_1-e_3}W). \tag{66}$$

Now using the Legendre relation $\eta_1w_2=-i\pi/2+\eta_2w_1$ and $k=\sqrt{e_2-e_3/e_1-e_3}=\sin\theta, k'=\cos\theta, q=\exp(\pi i w_3/w_1)$, we can obtain

$$X_+=-2\exp(4ir^2\overline{z})\int\sin\theta\,\mathrm{sn}(2rW)\mathrm{dn}(2rW)dW$$
$$=\exp(4ir^2\overline{z})\sin\theta\,\mathrm{cn}(2rW)/r,$$
$$X_3=\int[-1+2\,\mathrm{dn}(2rW)^2]dW$$
$$=-W+E(2rW|k)/r, \tag{67}$$

with the incomplete elliptic integral of the second kind E. Note that $W=z=\sigma$ in this case. This formula shows that the curve lies on a plane at a fixed time and this plane rotates around the z axis with the angular velocity $4r^2$. In Fig. 3, we show examples of the plane curve with $r=\frac{1}{2}$ and (a) $k=0.1$, (b) $k=0.85$. The curves make surfaces with the time $\pi/3<\overline{z}=\tau<2\pi/3$.

G. Point particle

The vortex filament coalesces into a point under the limit $\lambda_i\to\infty$. To describe this limit, we introduce $\Delta\to\infty$ such that $\lambda_i=\Delta\tilde{\lambda}_i$, $\sigma=\tilde{\sigma}/\Delta^2$, $\tau=\tilde{\tau}/\Delta^2$, for some finite $\tilde{\lambda}_i,\tilde{\sigma},\tilde{\tau}$. Then it is easy to find that $g_2=\Delta^4\tilde{g}_2$, $g_3=\Delta^6\tilde{g}_3$, $e_i=\Delta^2\tilde{e}_i$, where the notation should be obvious. The homogeneity relations of the Weierstrass functions give useful relations, $w_i=\tilde{w}_i/\Delta$, $\kappa_i=\tilde{\kappa}_i/\Delta$, $\eta_i=\Delta\tilde{\eta}_i$. We can check these relations as follows:

$$e_i=\mathcal{P}(\tilde{w}_i/\Delta,\Delta^4\tilde{g}_2,\Delta^6\tilde{g}_3)=\Delta^2\mathcal{P}(\tilde{w}_i,\tilde{g}_2,\tilde{g}_3)=\Delta^2\tilde{e}_i,$$

$$\eta_i=\zeta(\tilde{w}_i/\Delta,\Delta^4\tilde{g}_2,\Delta^6\tilde{g}_3)=\Delta\zeta(\tilde{w}_i,\tilde{g}_2,\tilde{g}_3)=\Delta\tilde{\eta}_i. \tag{68}$$

Using these relations, we can obtain

$$X_3=\frac{1}{\Delta}\left\{\frac{\tilde{s}_2\tilde{s}_1}{6\sqrt{\tilde{s}_4}}\tilde{\tau}-\frac{1}{2\sqrt{\tilde{s}_4}}\zeta(-\tilde{s}_1\tilde{\tau}+\tilde{w}_3,\tilde{g}_2,\tilde{g}_3)-\frac{\tilde{s}_3}{\sqrt{\tilde{s}_4}}\tilde{\tau}-\frac{\tilde{\eta}_3}{2\sqrt{\tilde{s}_4}}\right\},$$

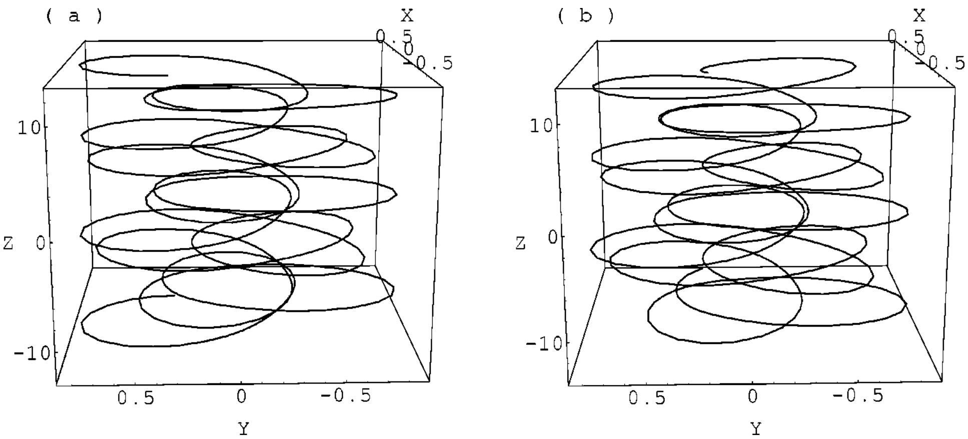

FIG. 4. (a) A typical open vortex filament at (a) $\tau=0$ with $-30<\sigma<30$ and (b) $\tau=0.5$ with $-30<\sigma<30$. The parameters of the filament are $\lambda_1=0.8+0.7i$, $\lambda_2=0.3+0.8i$.

$$\begin{aligned}X_+ = {} & \frac{i}{8\tilde{s}_4\Delta}\{\zeta(-\tilde{s}_1\tilde{\tau}+\tilde{w}_3+\tilde{\kappa}_1)-\zeta(-\tilde{s}_1\tilde{\tau}+\tilde{w}_3+\tilde{\kappa}_2)\\ & -\zeta(\tilde{\kappa}_1)+\zeta(\tilde{\kappa}_2)\},\\ & \times\frac{\sigma(-\tilde{s}_1\tilde{\tau}+\tilde{w}_3+\tilde{\kappa}_1)\sigma(-\tilde{s}_1\tilde{\tau}+\tilde{w}_3+\tilde{\kappa}_1)}{\sigma(-\tilde{s}_1\tilde{\tau}+\tilde{w}_3)^2\sigma(\tilde{\kappa}_1)\sigma(\tilde{\kappa}_2)}\\ & \times\exp\{\zeta(\tilde{\kappa}_1)\tilde{s}_1\tilde{\tau}+\zeta(\tilde{\kappa}_2)\tilde{s}_1\tilde{\tau}-\tilde{\eta}_3(\tilde{\kappa}_1+\tilde{\kappa}_2)+4i\sqrt{\tilde{s}_4}\tilde{\tau}\},\end{aligned} \tag{69}$$

which describes a point particle moving with the time $\tilde{\tau}$.

H. General vortex filament

Most generally, the solution in Eqs. (32) and (48) describes a vortex of open filament type. Figure 4 shows an example which we obtain using $\lambda_1=\lambda_3^*=0.8+0.7i,\lambda_2=\lambda_4^*=0.3+0.8i$. This is one of the most general configurations described by the one-phase periodic solution.

VI. CONCLUDING REMARKS

In this paper, we calculate the one-phase periodic solution of the localized induction approximation, which describes the motion of a thin vortex filament in an incompressible inviscid fluid. The solution was explicitly given in terms of Weierstrass elliptic functions. We study various vortex filament configurations resulting from the degenerate limit of the solution. It contains already known configurations such as the straight line, the Kelvin wave, the smoke ring, and the Hasimoto one-solitonic solution. In addition, it gives new configurations such as the rigid vortex filament, the closed string, the plane curve, and curling open filaments. Shigeo Kida was the first to introduce and investigate this category of vortex filament motion using an ansatz of a traveling wave [10]. But his solution is expressed in terms of elliptic integrals, having implicit parameters that are roots of a cubic equation. Compared to Kida's result, our solution via the elliptic functions has explicit parameters that are easy to manipulate. Moreover, our result is based upon a solid theoretical framework of the finite-band integration method, which offers the generalization to the case of N-phase periodic solutions.

The first appearance of Weierstrass elliptic functions in describing the vortex filament motion was in a work of Levi-Civita, see Eq. (66) of [5] or [17]. He used a slightly generalized version of the LIA to describe vortex filaments of uniform thickness. In his work, the local curvature $c(z)=R^{-1}(z)$ of stationary filaments was expressed in terms of Weierstrass' $\mathcal{P}$ function. It should be noticed that the equation was possible to be integrated by quadratures only for the case of stationary filament motions and the complete integrability of his equation is still not known. Thus it would be interesting to study the possibility of applying the method of the present paper to his equation and of obtaining vortex configurations of N phase periodic motions including N-solitons.

Another development in the study of vortex motion is due to Fukumoto, who investigated the three-dimensional configurations of a thin vortex filament embedded in background flows, based on the LIA [18]. He found some interesting configurations using an analogy between stationary configurations of a vortex filament in a steady flow with the trajectories of a charged particle in a steady magnetic field. Another analogy of the Kida class with a charged spherical pendulum in the field of a magnetic monopoles is also discussed and reproduces the result of Kida. It has the advantage of requiring less ingenuity to gain the integrals of motion by invoking the Lagrangian formalism of classical mechanics. But this method cannot be directly related to that of the present paper because, like Kida, it also uses an ansatz for vortex configurations to make the analogies. It would be interesting to find the possibility of complete integrability of motions which were shown to give closed expressions for vortex motions in background flows by Fukumoto.

Our formalism can be adapted to describe relativistic string dynamics in a uniform static field. It is described by the Lund-Regge model, $\ddot{X}-X''=X'\times\dot{X}$, which is the dynamical equation for a string $X(\tau,\sigma)$ [19]. Thus we can find string configurations of superfluid mechanics having quasiperiodic property. This will generalize previous works [20,22] which gives solitonic configurations using the duality between the Lund-Regge model and the complex sine-Gordon theory [23].

Using the result of Sec. III, we can obtain N-phase periodic solutions which should be described in terms of Riemann's theta functions. The difficulty in this program is the "effectivization" problem such that the obtained solution should satisfy Eq. (11). This, together with the difficulty in treating the Riemann θ function, would be the obstacle to apply it to real physical problems.

The stability analysis of the solution is another important physical problem to be done. A rather simple study was conducted using the perturbation method in [24]. Our formalism could be useful in that there exists a method for the analysis of long-time behavior of instabilities using the (quasi)periodic solution of the integrable system [13].

ACKNOWLEDGMENT

This work was supported by the Brain Korea 21 Project.

APPENDIX: DERIVATION OF THE LINEAR EQUATION

The derivation of the linear equation (7) needs the duality relation between the nonlinear Schrödinger equation and the localized induction approximation. We first start with the zero-curvature condition of the nonlinear Schrödinger equation,

$$[\partial - E - \lambda T, \bar{\partial} - T\partial E - ETE + 2\lambda E + 2\lambda^2 T] = 0, \quad \text{(A1)}$$

where $E = \begin{pmatrix} 0 & \psi \\ -\psi^* & 0 \end{pmatrix}$, $T = i\sigma_3$, and σ_3 is the Pauli matrix. The zero-curvature condition can be understood as the compatibility condition for the overdetermined system of equations

$$(\partial + U_{ns})\Phi = 0, \quad (\bar{\partial} + V_{ns})\Phi = 0, \quad \text{(A2)}$$

where $U_{ns} \equiv -\begin{pmatrix} 0 & \psi \\ -\psi^* & 0 \end{pmatrix} - \lambda T$ and $V_{ns} = -i\begin{pmatrix} |\psi|^2 & \partial\psi \\ \partial\psi^* & -|\psi|^2 \end{pmatrix} - \lambda\begin{pmatrix} 0 & -2\psi \\ 2\psi^* & 0 \end{pmatrix} + 2\lambda^2 T$. Equations (A2) and their compatibility condition (A1) have a natural geometric interpretation. In fact, the matrix functions U_{ns} and V_{ns} may be considered as local connection coefficients in the trivial bundle $R^2 \times C^2$ where the space-time R^2 is the base and the vector function Φ takes values in the fiber C^2. Equations (A2) show that Φ is a covariantly constant vector while Eq. (A1) amounts to saying that the (U_{ns}, V_{ns}) connection has zero curvature.

Now we introduce the duality relation by writing down the vortex variables X in Eq. (3) in terms of the nonlinear Schrödinger variables E and showing that the nonlinear Schrödinger equation (A1) implies the localized induction approximation (4). This can be achieved easily in terms of the associated linear equations in Eq. (A2) as follows: let $\Phi(z, \bar{z}, \lambda)$ be a solution of the linear equation of the nonlinear Schrödinger equation. Let us define a matrix F as

$$F \equiv \Phi^{-1} \frac{\partial}{\partial\lambda} \Phi. \quad \text{(A3)}$$

To check that it gives the localized induction approximation, we first notice that

$$\begin{aligned} \partial F &= -\Phi^{-1}\partial\Phi\Phi^{-1}\frac{\partial}{\partial\lambda}\Phi + \Phi^{-1}\frac{\partial}{\partial\lambda}(\partial\Phi) \\ &= -\Phi^{-1}\frac{\partial U_{ns}}{\partial\lambda}\Phi = \Phi^{-1}T\Phi. \end{aligned} \quad \text{(A4)}$$

In a similar way, we find that $\bar{\partial}F = -2\Phi^{-1}E\Phi - 4\lambda\Phi^{-1}T\Phi$ and $\partial^2 F = \Phi^{-1}[T,E]\Phi$. It is now easy to get a modified localized induction approximation,

$$\bar{\partial}F = \frac{1}{2}[\partial F, \partial^2 F] - 4\lambda\partial F. \quad \text{(A5)}$$

The localized induction approximation is obtained by taking $\lambda = 0$ in Eq. (A5). Thus we take $X = iF|_{\lambda=0}$ such that it satisfies the equation $\bar{\partial}X = [\partial X, \partial^2 X]/(2i)$. The constraint equation is automatically satisfied,

$$\mathrm{Tr}(\partial X)^2 = -TrT^2 = 2. \quad \text{(A6)}$$

We now use the modified form of the R transformation [14] to obtain the linear equation (7) of the localized induction approximation. First we define $\Psi \equiv \Phi^{-1}\hat{\Phi}$, where $\Phi(\hat{\Phi})$ is a solution of the linear equation (A2) with the spectral parameter $\lambda(\hat{\lambda})$. Define

$$\begin{aligned} M \equiv \partial\Psi\Psi^{-1} &= -\Phi^{-1}\partial\Phi + \Phi^{-1}\partial\hat{\Phi}\hat{\Phi}^{-1}\Phi \\ &= \Phi^{-1}(-E - \lambda T)\Phi + \Phi^{-1}(E + \hat{\lambda}T)\Phi \\ &= (\hat{\lambda} - \lambda)\partial F, \end{aligned}$$

$$\begin{aligned} N \equiv \bar{\partial}\Psi\Psi^{-1} &= 2(\lambda^2 - \hat{\lambda}^2)\Phi^{-1}T\Phi + 2(\lambda - \hat{\lambda})\Phi^{-1}E\Phi \\ &= 2(\lambda^2 - \hat{\lambda}^2)\partial F - (\lambda - \hat{\lambda})\bar{\partial}F - 4\lambda(\lambda - \hat{\lambda})\partial F. \end{aligned} \quad \text{(A7)}$$

Then the required linear equations are

$$(\partial - M)\Psi = 0, \quad (\bar{\partial} - N)\Psi = 0, \quad \text{(A8)}$$

which at $\lambda = 0$ becomes

$$[\partial + i\hat{\lambda}\partial X, \bar{\partial} - 2i\hat{\lambda}^2\partial X + i\hat{\lambda}\bar{\partial}X] = 0. \quad \text{(A9)}$$

Note that the compatibility condition of the linear equations, i.e., $[\partial - M, \bar{\partial} - N] = 0$ gives the localized induction approximation in a form of the zero-curvature condition. In the main text, we change $\hat{\lambda} \to \lambda$ for notational simplicity.

[1] L. S. Da Rios, Rend. Circ. Mat. Palermo **22**, 117 (1906).
[2] F. R. Hama, Phys. Fluids **5**, 1156 (1962); **6**, 526 (1963); R. J. Arms and F. R. Hama, *ibid.* **8**, 553 (1965).
[3] H. Hasimoto, J. Fluid Mech. **51**, 477 (1972).
[4] R. L. Ricca, Nature (London) **352**, 561 (1991).
[5] R. L. Ricca, Fluid Dyn. Res. **18**, 245 (1996).
[6] E. J. Hopfinger, F. K. Browand, and Y. Gagner, J. Fluid Mech. **125**, 505 (1982).
[7] T. Maxworthy, M. Mory, and E. J. Hopfinger, *Waves on Vortex Cores and their Relation to Vortex Breakdown*, AGARD Conference Proceedings No. 342 (Technical Editing and Reproduction Ltd., London, 1983), paper 29.
[8] D. Levi, A. Sym, and S. Wojciechowski, Phys. Lett. **94A**, 408 (1983).
[9] Y. Fukumoto and T. Miyazaki, J. Phys. Soc. Jpn. **55**, 4152 (1986).
[10] S. Kida, J. Fluid Mech. **112**, 397 (1981).
[11] See, for example, B. A. Dubrovin, I. M. Krichever, and S. P. Novikov, *Progress in Science and Engineering*, Contemporary Problems in Mathematics Vol. 4 (VINITI, Moscow, 1985).
[12] A. Sym, Fluid Dyn. Res. **3**, 151 (1988).
[13] E. R. Tracy and H. H. Chen, Phys. Rev. A **37**, 815 (1988).
[14] S. J. Orfanidis, Phys. Lett. **75A**, 304 (1980), and references therein.
[15] A. Kamchatnov, Phys. Rep. **286**, 199 (1997).
[16] *Encyclopedic Dictionary of Mathematics*, the Mathematical Society of Japan, edited by K. Itô (MIT Press, Cambridge, MA, 1993).
[17] T. Levi-Civita, Ann. R. Scuola Norm. Sup. Pisa **1**, 229 (1932).
[18] Y. Fukumoto, Proc. R. Soc. London, Ser. A **453**, 1205 (1997).
[19] F. Lund and T. Regge, Phys. Rev. D **14**, 1524 (1976).
[20] K. Lee, Q. Park, and H. J. Shin, Nucl. Phys. B **563**, 461 (1999).
[21] R. Betchov, J. Fluid Mech. **22**, 471 (1965).
[22] Q. Park and H. J. Shin, Phys. Lett. B **454**, 259 (1999).
[23] H. J. Shin, Nucl. Phys. B (to be published).
[24] S. E. Widnall, J. Fluid Mech. **54**, 641 (1972), and references therein.